Inorg. Chem. **2009**, *48*, 1000−1004

Peculiar High-Pressure Behavior of $BiMnO_3$

Alexei A. Belik,*,† Hitoshi Yusa,‡ Naohisa Hirao,§ Yasuo Ohishi,§ and Eiji Takayama-Muromachi†

International Center for Materials Nanoarchitectonics (MANA) and Advanced Nano Materials Laboratory (ANML), National Institute for Materials Science (NIMS), 1-1 Namiki, Tsukuba, Ibaraki 305-0044, Japan, and Synchrotron Radiation Research Institute (JASRI), 1-1-1 Kouto, Sayo-cho, 679-5198, Hyogo, Japan

Received August 22, 2008

High-pressure structural properties of perovskite-type $BiMnO_3$ have been investigated by synchrotron X-ray powder diffraction at room temperature. A new monoclinic phase having $P2_1/c$ symmetry was found between about 1.5 and 5.5 GPa. Above 8 GPa, the orthorhombic $GdFeO_3$-type phase (space group *Pnma*) is stable. The crystal structure of $BiMnO_3$ at 8.6 GPa and room temperature was investigated ($a = 5.5132(3)$ Å, $b = 7.5752(3)$ Å, $c = 5.4535(3)$ Å). The orthorhombic phase of $BiMnO_3$ has an orbital order similar to $LaMnO_3$ but with a different arrangement of orbitals in the *ac* plane. High-pressure room-temperature behavior of $BiMnO_3$ differs from high-temperature behavior at ambient pressure in comparison with $BiCrO_3$ and $BiScO_3$. These findings may open new directions in investigation of $BiMnO_3$.

1. Introduction

$BiMnO_3$[1−8] is one of the most studied multiferroic materials[9,10] among perovskite-type oxides together with $BiFeO_3$.[11] $BiMnO_3$ is a ferromagnet with $T_C = 100$ K,[5] and orbital degrees of freedom are active in $BiMnO_3$.[2] Ideal $BiMnO_3$ should crystallize in the centrosymmetric space group $C2/c$.[1] At ambient pressure (AP), three modifications of $BiMnO_3$ are known:[5] a room-temperature (RT) monoclinic $C2/c$ phase (phase I) with lattice parameters of $a = 9.5415(2)$ Å, $b = 5.61263(8)$ Å, $c = 9.8632(2)$ Å, $\beta = 110.6584(12)°$,[2,4,7] a high-temperature (HT) monoclinic $C2/c$ phase (phase II)[2,4,7] stable between 474 and 768 K, and an orthorhombic *Pnma* phase (O-phase) stable above 768 K up to the decomposition temperature. Orbital order exists in phase I, and it is believed that orbital order disappears in phase II.[2] The e_g orbitals of Mn^{3+} ions in phase I are arranged in such a way that there is only one kind of the e_g orbital within the plane (these planes are separated by $\sim c/4$) parallel to the *ab* plane. The following sequence $d_{z^2}/d_{x^2}/d_{z^2}/d_{y^2}/...$ is realized in phase I.[8] The crystal structure and the existence of orbital order in the O_{AP} phase of $BiMnO_3$ have not been investigated yet.

$BiCrO_3$ and $BiScO_3$ have the same structure with $BiMnO_3$.[12,13] However, $BiCrO_3$ and $BiScO_3$ adopt the phase II structure that is the orbital-disordered structure of $BiMnO_3$ because Cr^{3+} and Sc^{3+} are not orbitally active ions. $BiCrO_3$ shows one HT phase transition from phase II to O-phase at 420 K,[12,14] and $BiScO_3$ decomposes before this phase transition takes place.[2]

High-pressure (HP) behavior of $BiMO_3$ (M = Al, Sc, Cr, Mn, Fe, Co, Ga, and In) has been investigated poorly. HP behavior was studied in details only for $BiNiO_3$ because of the interesting pressure-induced intermetallic valence transition at 4 GPa from $Bi^{3+}_{0.5}Bi^{5+}_{0.5}Ni^{2+}O_3$ (having the *P*-1 symmetry) to $Bi^{3+}Ni^{3+}O_3$ (having the $GdFeO_3$-type orthor-

* To whom correspondence should be addressed. E-mail: Alexei.Belik@nims.go.jp.
† MANA, NIMS.
‡ ANML, NIMS.
§ JASRI.

(1) Baettig, P.; Seshadri, R.; Spaldin, N. A. *J. Am. Chem. Soc.* **2007**, *129*, 9854.
(2) Belik, A. A.; Iikubo, S.; Yokosawa, T.; Kodama, K.; Igawa, N.; Shamoto, S.; Azuma, M.; Takano, M.; Kimoto, K.; Matsui, Y.; Takayama-Muromachi, E. *J. Am. Chem. Soc.* **2007**, *129*, 971.
(3) Yokosawa, T.; Belik, A. A.; Asaka, T.; Kimoto, K.; Takayama-Muromachi, E.; Matsui, Y. *Phys. Rev. B* **2008**, *77*, 024111.
(4) Montanari, E.; Calestani, G.; Migliori, A.; Dapiaggi, M.; Bolzoni, F.; Cabassi, R.; Gilioli, E. *Chem. Mater.* **2005**, *17*, 6457.
(5) Kimura, T.; Kawamoto, S.; Yamada, I.; Azuma, M.; Takano, M.; Tokura, Y. *Phys. Rev. B* **2003**, *67*, 180401(R)
(6) Atou, T.; Chiba, H.; Ohoyama, K.; Yamaguchi, Y.; Syono, Y. *J. Solid State Chem.* **1999**, *145*, 639.
(7) Belik, A. A.; Takayama-Muromachi, E. *Inorg. Chem.* **2007**, *46*, 5585.
(8) Yang, C. H.; Koo, J.; Song, C.; Koo, T. Y.; Lee, K. B.; Jeong, Y. H. *Phys. Rev. B* **2006**, *73*, 224112.
(9) Ramesh, R.; Spaldin, N. A. *Nat. Mater.* **2007**, *6*, 21.
(10) (a) Azuma, M.; Takata, K.; Saito, T.; Ishiwata, S.; Shimakawa, Y.; Takano, M. *J. Am. Chem. Soc.* **2005**, *127*, 8889. (b) Hughes, H.; Allix, M. M. B.; Bridges, C. A.; Claridge, J. B.; Kuang, X.; Niu, H.; Taylor, S.; Song, W.; Rosseinsky, M. J. *J. Am. Chem. Soc.* **2005**, *127*, 13790.
(11) Wang, J.; Neaton, J. B.; Zheng, H.; Nagarajan, V.; Ogale, S. B.; Liu, B.; Viehland, D.; Vaithyanathan, V.; Schlom, D. G.; Waghmare, U. V.; Spaldin, N. A.; Rabe, K. M.; Wuttig, M.; Ramesh, R. *Science* **2003**, *299*, 1719.

10.1021/ic8015996 CCC: $40.75
Published on Web 01/07/2009

hombic structure).[15] HP structural behavior of $BiMnO_3$ at RT was studied in one work, however no phase transitions were identified up to 27 GPa probably because of low resolution of the energy-dispersive method used.[16] A few works appeared recently about HP behavior of $BiFeO_3$.[17] On the other hand, HP properties of $LaMnO_3$, a mother compound for a variety of magnetic and electric phases and colossal magnetoresistance materials, have been investigated in details in particular the stability of the Jahn−Teller distortion, metal−insulator transition, and magnetism.[18−20] The orbital order of $LaMnO_3$ has been much studied both experimentally and theoretically.[21,22]

In this work, we investigated HP structural properties of $BiMnO_3$ and compared them with those of $BiCrO_3$ and $BiScO_3$. All three compounds have the orthorhombic Gd-FeO_3-type structure above 8 GPa at RT, but $BiMnO_3$ shows interesting behavior at intermediate pressure. A new monoclinic phase was found between about 1.5 and 5.5 GPa, and the crystal structure of the orthorhombic phase of $BiMnO_3$ at 8.6 GPa was investigated where we found orbital order that is different from orbital order in $LaMnO_3$.

2. Experimental Section

Synthesis and Characterization of $BiMnO_3$. A stoichiometric mixture of Bi_2O_3 (99.99%) and Mn_2O_3 was placed in Au capsules and treated at 6 GPa in a belt-type high-pressure apparatus at 1383 K for 60−70 min.[2] After heat treatment, the samples were quenched to RT, and the pressure was slowly released. The resultant samples were black powder. X-ray powder diffraction (XRD) showed that the samples were single phase. Single-phase Mn_2O_3 was prepared by heating commercial MnO_2 (99.99%) in air at 923 K for 24 h. Bi_2O_3 was dried at 570 K before its use.

The careful structural analysis using high-resolution neutron powder diffraction data at different temperatures confirmed the stoichiometric composition of $BiMnO_3$.[2] In addition, the oxygen content of $BiMnO_3$ was determined by the thermogravimetric analysis. About 570 mg (to increase the accuracy) of $BiMnO_3$ was placed into an Al_2O_3 crucible, heated in 3 h up to 873 K, and kept for 1 h at 873 K in 100% H_2. The experimental weight loss gave the following composition $BiMnO_{3.01(1)}$.

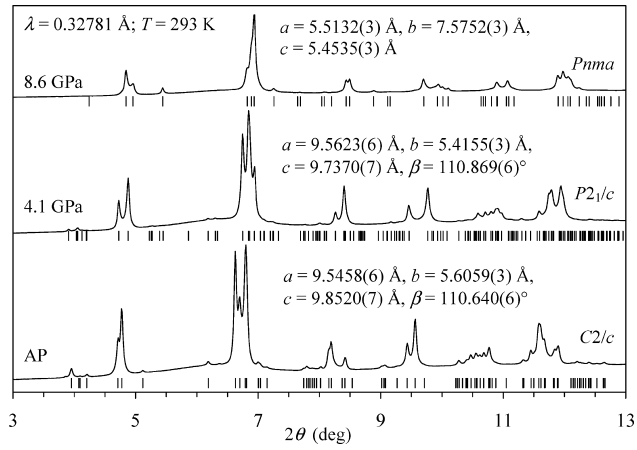

Figure 1. Synchrotron X-ray powder diffraction patterns of $BiMnO_3$ at room temperature and ambient pressure, 4.1 GPa, and 8.6 GPa. The allowed Bragg reflections for the corresponding space groups are indicated by tick marks. The refined lattice parameters are given.

Synchrotron X-ray Powder Diffraction (SXRD) Experiments at High Pressure. A symmetric diamond anvil cell (DAC), equipped with a culet diameter of 0.4 mm, was used for the high-pressure experiments. The powder $BiMnO_3$ sample was put into a chamber (0.15 mm in diameter) in a rhenium gasket (0.8 mm in thickness) with a few small grains of ruby (less than 5 μm) to measure pressure.[23] The sample was immersed in a pressure medium (methanol/ethanol/water = 16:3:1) to present a hydrostatic condition. The in situ XRD experiments were performed at RT on BL04B2 at SPring-8.[24] A monochromatic X-ray beam (38 keV) was focused and collimated to the sample within 50 μm size. Diffracted X-rays were detected by an imaging plate (IP). The distance from the IP to the sample was kept as long as possible (L = 640.010) in the X-ray diffractometer so that a high-energy X-ray (λ = 0.32781 Å) could be used to get an accurate value for d. Typical exposure time was 20 min. Diffraction patterns were collected with increasing pressure up to 8.7 GPa at intervals of ∼1−2 GPa. After that, the patterns in decompression process were taken. In this pressure range, the hydrostaticity was completely kept because no freezing of the pressure medium was observed under an optical microscope. Diffraction data were analyzed by the Rietveld method with *RIETAN-2000*.[25]

3. Results and Discussion

At AP, all Bragg reflections in the SXRD patterns of $BiMnO_3$ can be indexed in space group $C2/c$. Already at 0.9 GPa, we observed the appearance of new reflections (Supporting Information). The careful analysis showed the appearance of the second monoclinic phase, which we will call the P-phase. At 2.5 and 4.1 GPa, only the P-phase was found. At 6.0 GPa, we observed the appearance of other additional reflections from the O-phase (Supporting Information). P- and O-phases coexisted up to 7.4 GPa, and only the O-phase was observed at 8.6 GPa. Figure 1

(12) Belik, A. A.; Iikubo, S.; Kodama, K.; Igawa, N.; Shamoto, S.; Takayama-Muromachi, E. *Chem. Mater.* **2008**, *20*, 3765.
(13) Belik, A. A.; Iikubo, S.; Kodama, K.; Igawa, N.; Shamoto, S.; Maie, M.; Nagai, T.; Matsui, Y.; Stefanovich, S. Yu.; Lazoryak, B. I.; Takayama-Muromachi, E. *J. Am. Chem. Soc.* **2006**, *128*, 706.
(14) Niitaka, S.; Azuma, M.; Takano, M.; Nishibori, E.; Takata, M.; Sakata, M. *Solid State Ionics* **2004**, *172*, 557.
(15) Azuma, M.; Carlsson, S.; Rodgers, J.; Tucker, M. G.; Tsujimoto, M.; Ishiwata, S.; Isoda, S.; Shimakawa, Y.; Takano, M.; Attfield, J. P. *J. Am. Chem. Soc.* **2007**, *129*, 14433.
(16) Chi, Z. H.; You, S. J.; Yang, L. X.; Chen, L. C.; Jin, C. Q.; Wang, X. H.; Chen, R. Z.; Li, L. T.; Li, Y. C.; Li, X. D.; Liu, J. *J. Electroceram.,* DOI 10.1007/s10832−007−9306−0.
(17) Gavriliuk, A. G.; Struzhkin, V. V.; Lyubutin, I. S.; Troyan, I. A. *JETP Lett.* **2007**, *86*, 197.
(18) Fuhr, J. D.; Avignon, M.; Alascio, B. *Phys. Rev. Lett.* **2008**, *100*, 216402.
(19) Loa, I.; Adler, P.; Grzechnik, A.; Syassen, K.; Schwarz, U.; Hanfland, M.; Rozenberg, G. Kh.; Gorodetsky, P.; Pasternak, M. P. *Phys. Rev. Lett.* **2001**, *87*, 125501.
(20) Pinsard-Gaudart, L.; Rodriguez-Carvajal, J.; Daoud-Aladine, A.; Goncharenko, I.; Medarde, M.; Smith, R. I.; Revcolevschi, A. *Phys. Rev. B* **2001**, *64*, 064426.
(21) Shen, Q.; Elfimov, I. S.; Fanwick, P.; Tokura, Y.; Kimura, T.; Finkelstein, K.; Colella, R.; Sawatzky, G. A. *Phys. Rev. Lett.* **2006**, *96*, 246405.
(22) Rodríguez-Carvajal, J.; Hennion, M.; Moussa, F.; Moudden, A. H.; Pinsard, L.; Revcolevschi, A. *Phys. Rev. B* **1998**, *57*, 3189(R)
(23) Mao, H. K.; Xu, J.; Bell, P. M. *J. Geophys. Res.* **1986**, *91*, 4673–4676.
(24) Kohara, S.; Itou, M.; Suzuya, K.; Inamura, Y.; Sakurai, Y.; Ohishi, Y.; Takata, M. *J. Phys.: Condens. Matter* **2007**, *19*, 506101.
(25) Izumi, F.; Ikeda, T. *Mater. Sci. Forum* **2000**, *321−324*, 198.

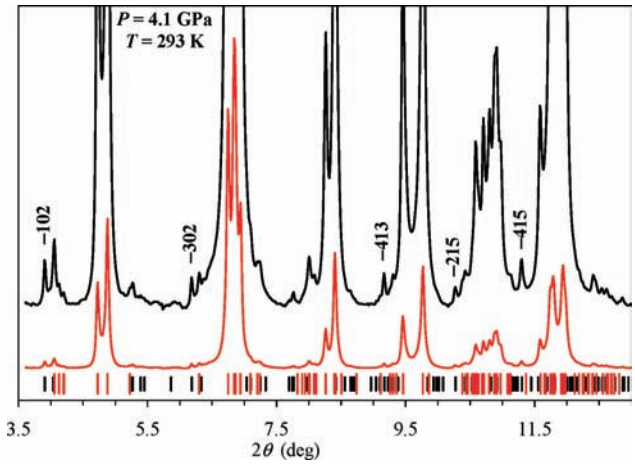

Figure 2. Synchrotron X-ray powder diffraction pattern of $BiMnO_3$ at room temperature and 4.1 GPa. The background is subtracted for clarity. The full (red) and enlarged (black) patterns are shown. The long red tick marks show positions of Bragg reflections for space group $C2/c$. The short black tick marks show the positions of additional Bragg reflections for space group $P2_1/c$. Indices of some strongest additional reflections, which break the C-centered monoclinic cell, are given.

depicts the SXRD patterns of $BiMnO_3$ at AP, 4.1 GPa, and 8.6 GPa.

Indexing Bragg reflections of the P-phase revealed it to crystallize in a monoclinic system with lattice parameters of $a = 9.5903(9)$ Å, $b = 5.4425(4)$ Å, $c = 9.7802(10)$ Å, and $\beta = 110.940(8)°$ at 2.5 GPa. Reflection conditions derived from the indexed reflections of the P-phase were $l = 2n$ for $h0l$, $h00$, and $00l$ and $k = 2n$ for $0k0$, affording one possible space group $P2_1/c$ (No. 14).[26] Because this space group is centrosymmetric, it cannot support ferroelectricity. We should emphasize that it is the maximum possible space group because some observed reflection conditions may be broken if the corresponding reflections are very weak or overlap with other reflections.

P-phase is very similar to phase I (space group $C2/c$) except for breaking the C-centered monoclinic cell (Figure 2). At 0.9 GPa, the refined lattice parameters were $a = 9.5057(13)$ Å, $b = 5.5726(6)$ Å, $c = 9.7974(14)$ Å, and $\beta = 110.458(12)°$ for phase I and $a = 9.6342(13)$ Å, $b = 5.4648(5)$ Å, $c = 9.8191(14)$ Å, and $\beta = 111.040(12)°$ for P-phase. That is, the a and c parameters and β angle increase, and the b parameter decreases during this HP phase transition (insets of Figure 3). The unit cell volume shrinks during the phase I ⟹ P-phase and P-phase ⟹ O-phase transitions as expected for HP phase transitions (Figure 3). During the temperature-driven[5] and composition-driven (in $BiMn_{1-x}M_xO_3$ with M = Al, Sc, Cr, Fe, and Ga)[7,27] phase I ⟹ phase II transition at AP, the a parameter increases, and the b and c parameters and β angle decrease. In other words, the phase I ⟹ P-phase transition is obviously different from the phase I ⟹ phase II transition.

In the case of $BiCrO_3$ and $BiScO_3$, the P-phase was not detected (Figure 4). Phase II of $BiCrO_3$ and $BiScO_3$

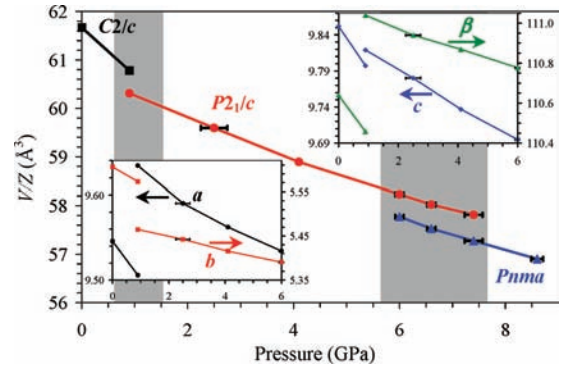

Figure 3. Pressure dependence of unit cell volume V divided by Z (Z is the number of formula units per unit cell) in $BiMnO_3$ at room temperature (during increase of pressure). Grey rectangles show the two-phase regions. Insets depict the pressure (in GPa) dependence of the lattice parameters (Å for the parameters and deg for the angle) of phase I and P-phase. Errors along y axes are smaller than the symbols.

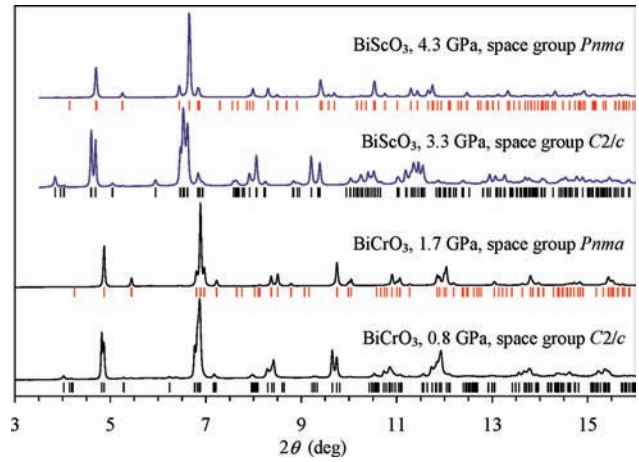

Figure 4. Synchrotron X-ray powder diffraction patterns of $BiCrO_3$ and $BiScO_3$ at room temperature and different pressure. The long tick marks show positions of Bragg reflections.

transforms to O-phase starting from ca. 1 and 3.7 GPa, respectively. The HP-RT behavior of $BiCrO_3$ and $BiScO_3$ resembles the AP-HT behavior of these compounds even though the effects of pressure and temperature are different. During the compression, the unit cell parameters and volume shrink, whereas on heating the unit cell parameters and volume usually expands. In $BiCrO_3$, the phase II ⟹ O-phase transition occurs at 420 K at AP and at 1 GPa at RT. In $BiScO_3$, the phase II ⟹ O-phase transition should occur above 980 K at AP, and it occurs at a higher pressure of 3.7 GPa at RT. However, the HP-RT behavior of $BiMnO_3$ differs from the AP-HT behavior. At AP, the following sequence occurs: phase I ⟹ phase II ⟹ O_{AP}-phase.[2,4,5,27] At HP, we observed phase I ⟹ P-phase ⟹ O_{HP}-phase. That is, intermediate phases are different, whereas the final phases of $BiMnO_3$ seem to be the same. We should emphasize that we could not detect phase II in the HP experiments on $BiMnO_3$.

The appearance of the P-phase (where the C-centered cell is surely broken) at moderate pressure can also explain the observation of very weak and broad reflections $h0l$ with $h = 2n + 1$ (forbidden in $C2/c$) on the selected-area electron diffraction patterns of $BiMnO_3$ at AP and RT.[3] In other words, domains of the P-phase or stress caused by the

(26) Hahn, T. *International Tables for Crystallography*, 5th ed.; Kluwer: Dordrecht, The Netherlands, 2002; Vol. *A*, p 52.
(27) Belik, A. A.; Yokosawa, T.; Kimoto, K.; Matsui, Y.; Takayama-Muromachi, E. *Chem. Mater.* **2007**, *19*, 1679.

Table 1. Structure Parameters of $BiMnO_3$ at RT and 8.6 GPa[a]

site	Wyckoff position	*x*	*y*	*z*	*B* (Å^2)
Bi	4*c*	0.0368(3)	0.25	0.9953(12)	0.19(6)
Mn	4*b*	0	0	0.5	0.2(10)
O1	4*c*	0.453(4)	0.25	0.043(10)	1.0
O2	8*d*	0.301(4)	0.027(3)	0.645(4)	1.0

[a] Space group *Pnma* (No 62); $Z = 4$; $a = 5.5132(3)$ Å, $b = 7.5752(3)$ Å, $c = 5.4535(3)$ Å, and $V = 227.76(2)$ Å^3, $R_{wp} = 2.03\%$, $R_p = 1.42\%$, $R_B = 1.32\%$, and $R_F = 0.76\%$. The occupation of all of the sites is unity. The *B* parameters for oxygen were fixed.

Table 2. Bond Lengths in $BiMnO_3$ at RT and 8.6 GPa and in $LaMnO_3$ at RT and AP[22]

distance (Å)	$BiMnO_3$	$LaMnO_3$
Mn−O1 (×2)	1.93(1)	1.968
Mn−O2 (×2)	1.85(2)	2.180
Mn−O2 (×2)	2.23(2)	1.906
Bi/La−O2 (×2)	2.27(2)	2.459
Bi/La−O2 (×2)	2.42(3)	2.698
Bi/La−O2 (×2)	2.94(3)	2.650
Bi/La−O1	2.31(2)	2.560
Bi/La−O1	2.56(5)	2.425
Bi/La−O1	2.97(5)	3.158
Bi/La−O1	3.23(5)	3.260

P-phase may exist at AP and RT especially taking into account noticeable hysteretic behavior during the pressure release (for example, a mixture of P- and O-phases was observed at 4 GPa during the decompression process).

The reflections that break the *C*-centered cell in the P-phase are very weak, and the number of refined structural parameters is large in the $P2_1/c$ model. Therefore, attempts to get reliable structural parameters for the P-phase from SXRD failed.

On the other hand, the crystal structure of the O_{HP}-phase of $BiMnO_3$ at 8.6 GPa and RT could be successfully refined. Structure parameters of $LaMnO_3$[22] in space group *Pnma* were used as initial ones in the Rietveld refinement of $BiMnO_3$. Coefficients for analytical approximation to atomic scattering factors for Bi, Mn, and O were taken from ref 28. The pseudo-Voigt function of Toraya was used as a profile function.[29] The background was represented by a composite background function, that is the 11th-order Legendre polynomial multiplied by a set of numerical values to approximate the background. The occupancy factor, *g*, of all the sites was unity ($g = 1$). Isotropic atomic displacement parameters, *B*, with the isotropic Debye–Waller factor represented as $\exp((-B \sin^2 \theta)/\lambda^2)$ were assigned to all of the sites. Final lattice parameters, *R* factors, fractional coordinates, *B* parameters, and some bond lengths of $BiMnO_3$ at 8.6 GPa and RT are listed in Tables 1 and 2. Figure 5 displays observed, calculated, and difference SXRD patterns.

Structural studies of the O_{HP}-phase of $BiMnO_3$ showed that there is strong Jahn−Teller distortion with two long Mn−O2 bond lengths and, therefore, the orbital order (inset of Figure 5 and Table 2). The crystal structure of the O_{HP}-phase of $BiMnO_3$ is very similar with that of $LaMnO_3$ at AP and RT. However, the O2 atom in $BiMnO_3$ (*x*, *y*, *z* = 0.301, 0.027, 0.645) exhibits a noticeable shift along the *c* axis compared with the position of the O2 atom in $LaMnO_3$ (*x*, *y*, *z* = 0.307, 0.038, 0.726).[22] The origin of this shift is the presence of a lone electron pair of a Bi^{3+} ion. With this O2 shift, two Bi−O2 bond lengths (2.27 Å) became much shorter than the corresponding La−O2 bond lengths (2.46 Å), and two other Bi−O2 bond lengths (2.94 Å) became much longer than the La−O2 bond lengths (2.65 Å) (Table 2). The resulting oxygen coordination of Bi^{3+} is very typical for this ion. The same coordination was observed, for example, in $BiMnO_3$ at AP[2] and in $BiNiO_3$ at AP and 7.7 GPa.[15] We note that space group *Pnma* is centrosymmetric and does not support ferroelectricity.

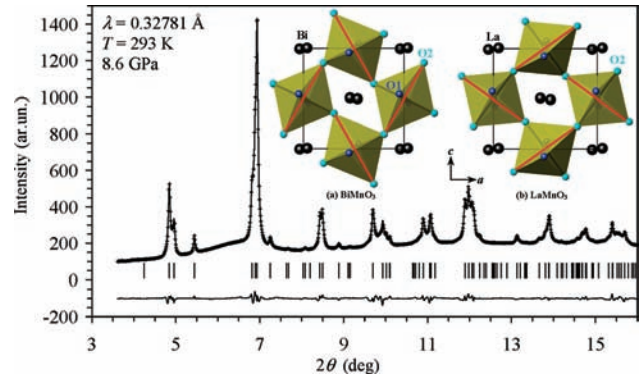

Figure 5. Fragments of observed (crosses), calculated (solid line), and difference patterns resulting from the Rietveld analysis of the synchrotron X-ray powder diffraction data for $BiMnO_3$ at 8.6 GPa and room temperature. Bragg reflections are indicated by tick marks. The inset gives projections of the crystal structures of $BiMnO_3$ (at 8.6 GPa and room temperature) and $LaMnO_3$ (at ambient pressure and room temperature)[22] along the *b* axis. The longest Mn−O2 bond lengths are marked with bold (red) lines.

$LaMnO_3$ crystallizes in the so-called O'-orthorhombic structure at AP and RT ($a = 5.7473$ Å, $b = 7.6929$ Å, $c = 5.5367$ Å in space group *Pnma*).[22] The O' structure has $a > c > b/\sqrt{2}$. The O' structure is related to cooperative ordering of the occupied e_g orbitals. There is also another orthorhombic structure (O) found in $LaMnO_{3+\delta}$ or $LaMn_{1-x}Ga_xO_3$ with $x > 0.5$ where the orbital order disappears.[30,31] The O structure has $c > a \approx b/\sqrt{2}$.[31] The O_{HP}-phase of $BiMnO_3$ has $a > c > b/\sqrt{2}$ and, therefore, belongs to the O'-structure type with orbital ordering.

There is an interesting effect of the shift of the O2 atom in $BiMnO_3$, namely, change of the orbital ordering pattern in $BiMnO_3$ compared with that of $LaMnO_3$ (inset of Figure 5). The orbitals lie in the *ac* plane (in *Pnma*) in both cases. However, the direction of the longest Mn−O2 bond lengths in $BiMnO_3$ is almost orthogonal with that of $LaMnO_3$ (using exactly the same projection of the crystal structures in space group *Pnma* with $a > c > b/\sqrt{2}$). There is only one kind of e_g orbital within the plane (these planes are separated by $c/2$) parallel to the *ab* plane.[18] The following sequence $d_{z^2}/d_{x^2}/...$ is realized in the O_{HP}-phase of $BiMnO_3$, which is different from the staking sequence in phase I of $BiMnO_3$.[8] In principle, the magnetic and structural properties of the

(28) Wilson, A. J. C.; Prince, E. *International Tables for Crystallography*, 2nd ed.; Kluwer: Dordrecht, The Netherlands, 1999; Vol. C, pp 572−574.
(29) Toraya, H. *J. Appl. Crystallogr.* **1990**, *23*, 485.
(30) Huang, Q.; Santoro, A.; Lynn, J. W.; Erwin, R. W.; Borchers, J. A.; Peng, J. L.; Greene, R. L. *Phys. Rev. B* **1997**, *55*, 14987.
(31) Blasco, J.; Garcia, J.; Campo, J.; Sanchez, M. C.; Subias, G. *Phys. Rev. B* **2002**, *66*, 174431.

O_{HP}-phase of $BiMnO_3$ should be similar to those of $LaMnO_3$ because they are isostructural. In $LaMnO_3$, for example, the Jahn−Teller distortion is completely suppressed above 18 GPa at RT, a metal−insulator transition takes place above 32 GPa at RT,[19] and spins of Mn^{3+} start to rotate above 6.7 GPa at low temperatures.[20] However, the different orbital ordering pattern of $BiMnO_3$ and different behavior of Bi^{3+} (with a lone electron pair) under pressure may have unexpected effects.

It is interesting to note that $BiCrO_3$, $BiScO_3$, $BiMnO_3$, and $BiNiO_3$[15] end up at the orthorhombic $GdFeO_3$-type phase, at least, up to 8−10 GPa and at RT. Theoretical investigations also predicted the $GdFeO_3$-type phase for $BiFeO_3$ at HP.[32] $LaCrO_3$, $LaScO_3$, $LaMnO_3$, and $LaFeO_3$ crystallize in the orthorhombic $GdFeO_3$-type structure at AP and RT. Therefore, pressure seems to remove structural distortions caused by the presence of a lone electron pair of Bi^{3+}.

The recent first-principle calculations on $BiMnO_3$ showed that there is strong competition between the ferromagnetic state (with the $C2/c$ symmetry) and the ↑↓↓↑ antiferromagnetic state due to the peculiar geometry of the orbital ordering pattern in $BiMnO_3$ at AP and RT and effects of next-nearest-neighbor interactions.[33] The ↑↓↓↑ antiferromagnetic state breaks the C-centered monoclinic cell. Pressure may change the balance between the nearest-neighbor/next-nearest-neighbor and ferromagnetic/antiferromagnetic interactions and stabilize a new monoclinic phase. In any case, the appearance of the P-phase at pressures as low as 0.9 GPa shows that phase I is rather unstable, in agreement with the first principle calculations,[33] and small variations of external parameters may stabilize a different phase.

In conclusion, we found a new monoclinic phase of $BiMnO_3$, which emerged at pressures as low as 0.9 GPa, and investigated the crystal structure of the orthorhombic phase of $BiMnO_3$ at 8.6 GPa. The orbital order exists in the orthorhombic phase similar to $LaMnO_3$ but with a different orbital ordering pattern. We hope that our findings will open new directions in the investigation of $BiMnO_3$. For example, interesting questions are (1) magnetic properties of P- and O_{HP}-phases,[34] (2) stability of the Jahn−Teller distortion of the O_{HP}-phase, (3) crystal structure analysis of the P-phase using neutron diffraction and understanding the orbital order of the P-phase, (4) theoretical understanding of the P-phase and peculiar HP behavior of $BiMnO_3$, and (5) existence of orbital order in the O_{AP}-phase of $BiMnO_3$ (above 768 K) and comparison of O_{HP}- and O_{AP}-phases.

Acknowledgment. This work was partially supported by World Premier International Research Center Initiative (WPI Initiative, MEXT, Japan). We thank Dr. T. Kolodiazhnyi of NIMS for the TG analysis in hydrogen.

Supporting Information Available: Details of SXRD patterns of $BiMnO_3$. This material is available free of charge via the Internet at http://pubs.acs.org.

IC8015996

(32) Ravindran, P.; Vidya, R.; Kjekshus, A.; Fjellvag, H.; Eriksson, O. *Phys. Rev. B* **2006**, *74*, 224412.
(33) Solovyev, I. V.; Pchelkina, Z. V. *New J. Phys.* **2008**, *10*, 073021.
(34) Chou, C. C.; Taran, S.; Her, J. L.; Sun, C. P.; Huang, C. L.; Sakurai, H.; Belik, A. A.; Takayama-Muromachi, E.; Yang, H. D. *Phys. Rev. B* **2008**, *78*, 092404.